International Journal of Nanoelectronics and Materials
Volume 15, No. 1, January 2022 [17-26]

Structural, Optical Properties and Raman Spectroscopy of In_2O_3 Doped $LiTaO_3$ Thin Films

Nani Djohan[1*], Budi Harsono[1], Johansah Liman[1], Hendradi Hardhienata[2] and Irzaman[2*]

[1] Department of Electrical Engineering, Faculty of Engineering and Computer Science, Universitas Kristen Krida Wacana, Jl. Tj. Duren Raya No. 4, Jakarta 11470, Indonesia
[2] Department of Physics, Faculty of Mathematics and Natural Sciences, Bogor Agricultural University, Jl. Raya Dramaga, Bogor 16680, Indonesia

Received 8 March 2021, Revised 22 April 2020, Accepted 28 April 2021

ABSTRACT

In this experiment, undoped, 2 wt.%, 4 wt.% and 6 wt.% In_2O_3 doped $LiTaO_3$ thin films were successfully prepared by utilizing a spin coater to carry out chemical solution deposition on the substrate surface (CSD method). The films were grown on the p-type Si (100) substrates with 2 M in 2-methoxyethanol precursor, whose solubility was twisted at 4000 rpm for 30 seconds. Crystalline formation of the films was carried out at annealing temperature 850 ^oC, held for 15 hours at a temperature rise rate of 1.67 ^oC/min. In term of XRD analysis, the structural properties of $LiTaO_3$ thin film undergo increment in crystallite size and lattice parameter values as the concentration of indium doping increase. The optical properties and Raman spectra of the films were then obtained using UV-Vis spectrometer and Raman spectroscopy. From the XRD measurement, the result shows a hexagonal crystal structure with lattice parameters a = 5.032-5.051 Å and c = 13.643-13.676 Å, and from the UV-Vis data, we observed that the films have a 5.034-5.184 Ev energy gap with 1.70364373 – 1.70364377 refractive index. Raman analysis produces peaks of $LiTaO_3$, A_1TO_{10} (In_2O_3) and A_1LO_{10} (In_2O_3). Based on the characterization results, it can be concluded that the 6 wt% In_2O_3 doped $LiTaO_3$ thin films are very promising for application as a light sensor.

Keywords: $LiTaO_3$, In_2O_3, x-ray diffraction, Raman spectroscopy, uv-vis spectroscopy

1. INTRODUCTION

A thin film made from Lithium tantalate ($LiTaO_3$) is an essential optical material, mainly due to its excellent electro/acousto-optical properties, high electro-optic and pyroelectric coefficient of 30.5 pm/V and 230 $\mu C, m^{-2}.s^{-1}$ respectively, and high curie temperature of 655 ^oC [1,2]. The thickness of the sensitive cells is inversely proportional to the detector response [3-5]. $LiTaO_3$ is very attractive and promising material for optical sensor [3,7]. The performance of thin films can be increased by the addition of doping materials. The concentration of the doping materials affects the structural and optical properties of the thin films. Mendoza et al. [8] deposited Fe-doped $LiTaO_3$ thin films by magnetron sputtering and they investigated the effect of iron doping on the crystalline structure. Irzaman et al. [14] prepared lanthanum doped $LiTaO_3$ thin films by CSD method and they investigated the effect of dopant addition on the crystal formation and the optical properties of the films.

There are various kinds of technology to synthesize $LiTaO_3$ thin films. X-ray Diffraction (XRD) technology is based on diffraction of X-Ray when scattering light with a wavelength passing through a crystal lattice with a distance between crystal fields. Previous study stated on the crystal structure and lattice parameter found that the diffraction angle depends on the gap of the

*Corresponding author: nani.djohan@ukrida.ac. irzaman@apps.ipb.ac.id

lattice width, thus affecting the diffraction pattern [12]. In contrast, the diffraction light intensity depends on the number of crystal lattices having the same orientation. Crystal system, parameter of the lattice, the degree of crystallinity, structure type, and orientation can be determined by this method. $LiTaO_3$ thin film with high purity and best intensity was selected from the XRD measurement [3,9,10].

Solid-state and molecule vibrational properties can be analyzed by using Raman spectroscopy [11,12]; thus, strain [12,15], doping [12,16,17], stoichiometry [12,13,14] and crystallinity property information can be obtained by this technology. Density functional theory (DFT) is the combination of Raman with theoretical approaches yielding phonon eigenvectors [12]. In this experiment, four types of solution ($LiTaO_3$, $LiTaO_3$ + 2 wt.% In_2O_3, $LiTaO_3$ + 4 wt.% In_2O_3, and $LiTaO_3$ + 6 wt.% In_2O_3) were produced and structural, optical properties and raman spectra were carried out.

2. MATERIAL AND METHODS

The p-type Si (100) substrates cut in size of 1x1 cm^2 were ultrasonically cleaned in acetone (C_3H_6O) and repeated sequentially using methanol (CH_3OH) and deionized water successively for 15 minutes [5,9,24-27]. The undoped $LiTaO_3$ solution was prepared by dissolving 0.5897 gram of lithium tantalate (≥99.99%, Sigma-Aldrich 704393-5G) in 2.5 ml of 2-methoxyethanol. The 2 wt.%, 4 wt.%, and 6 wt.% In_2O_3 doped $LiTaO_3$ solutions were prepared by dissolving 0.5897 gram of lithium tantalate and 0.01179 gram, 0.0236 gram, and 0.03538 gram of indium (III) oxide (99.99%, Sigma-Aldrich 289418-10G), respectively in 2.5 ml of 2-methoxyetanol.

To get the homogeneous $LiTaO_3$ solution, it was stirred using Vortex 3000 mixer and then sonicated using an ultrasonicator device (J.P Selecta) for 30 minutes [5,9]. Furthermore, the thin films were deposited on the p-type Si (100) substrates using spin coater for 30 seconds using a rotating speed of 4000 rpm. This process was repeated three times with a one-minute time interval [5,6,9,19,24-29]. The annealing process was done using Nabertherm B410 furnace at temperature 850^{o}C for 15 hours, with a temperature increment speed of 1.67^{o}C/min. The structural properties of the thin-film crystal were then obtained with an X-Ray Diffractometer (Bruker D2 PHASER) with the interval of 2 theta angles from 20 to 80 degrees with a 0.02 degrees step, where thin films have formed crystals at specific angular peaks with hexagonal-shaped crystal structures. Furthermore, the thin films were characterized by using a UV-Vis spectrometer (Ocean Optics USB4000-UV-Vis) and Raman spectroscopy (Horriba iHR550) to investigate the transversal and longitudinal phonon modes of the films [11,12,18,20-23].

3. RESULTS AND DISCUSSION

3.1 Structural properties

The XRD patterns of $LiTaO_3$ thin films were determined from $20^{o} \leq 2\theta \leq 80^{o}$ intervals with a scanning rate of 0.02^{o}/minute [9,14,30-32]. Figure 1 shows the XRD patterns of undoped and In_2O_3 doped $LiTaO_3$ thin films [9,14,30]. The Miller index values were assigned by referring to the standard x-ray diffraction powder patterns file (JCPDS Natl Bur, 1977) and were in good agreement with the values reported in the file. From the Rietveld refinement result, the Goodness of Fit (GOF) for the undoped and In_2O_3 doped $LiTaO_3$ thin films varies between 1.39 and 2.91. The Weighted R profile (R_{wp}), expected R profile (R_{exp}) and GOF are given in Table 1. The XRD patterns showed that $LiTaO_3$ thin films were both amorphous and crystalline with hexagonal crystal structure. The percentage of amorphous and crystalline are given by the crystallinity index (CI) in the Table 1. All the XRD patterns showed a preferred strong peak at (012) diffraction plane. The peaks profiles of the two most dominant peaks at (012) and (104) diffraction plane was obtained by Gaussian fitting. Peak position (2θ) and the full width at half maximum (FWHM) from the peaks are shown in Table 2.

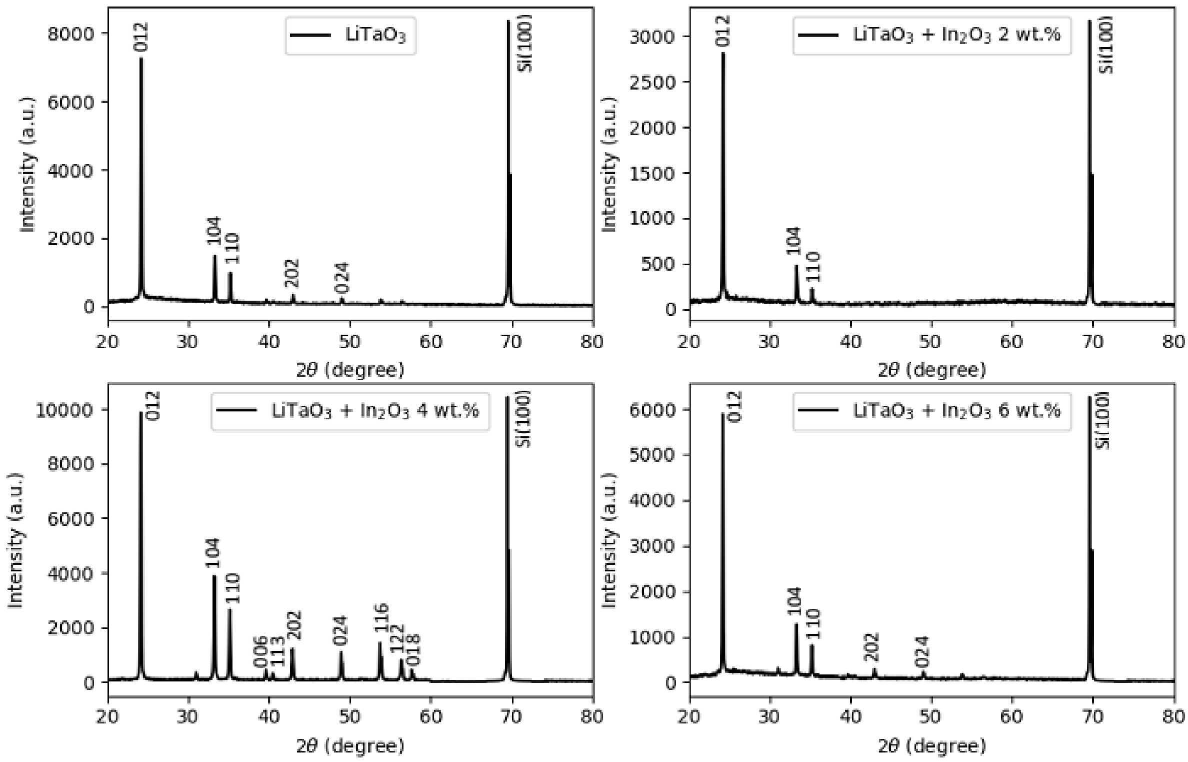

Figure 1. XRD patterns of $LiTaO_3$ thin films with different doped In_2O_3 at annealing temperature 850°C

The crystallite size (D) of the undoped and In_2O_3 doped $LiTaO_3$ thin films was calculated using Debye Scherer's formula:

$$D = \frac{k\lambda}{\beta cos\theta} \tag{1}$$

where k is the shape factor (= 0.9), λ is the X-ray radiation wavelength (= 0.15406 nm), β is FWHM of diffraction peak in radian, and θ is the Bragg's diffraction angle in radian. The highest crystallite size values observed were 51.408 nm and 46.620 nm for (012) and (104) diffraction plane in 6 wt.% In_2O_3 doped $LiTaO_3$ thin film, respectively. The crystallite size decreased in line with the decrease in doping concentration, as shown in Table 2. The decrease of crystallite size may be due to better integration of In_2O_3 ion into the $LiTaO_3$ structure [38].

The dislocation density (δ) of the undoped and In_2O_3 doped $LiTaO_3$ thin films could be obtained using the Williamson-Smallman formula:

$$\delta = \frac{1}{D^2} \tag{2}$$

where D is the crystallite size of the films obtained from Eq. 1. It was observed that the dislocation density decreases as doping concentration increases.

The lattice strain (ε) of the undoped and In_2O_3 doped $LiTaO_3$ thin films was calculated by using the following formula:

$$\varepsilon = \frac{\beta}{4 \tan \theta} \tag{3}$$

The data show that when doping concentration increases beyond 2 wt.%, lattice strain will decrease. This suggests the creation of fewer defects in the $LiTaO_3$ lattice. The same finding was obtained by Sahoo et al. [39] in indium doped ZnO thin films. All the calculated results from the XRD data are shown in Table 2.

The interplanar spacing (d_{hkl}) for each peak can be calculated using Bragg's formula, as shown in Eq. 4. The lattice parameters (a and c) can be calculated from the interplanar spacing equation for hexagonal lattice as shown in Eq. 5, where hkl is the Miller indices of the plane of diffraction.

$$d_{hkl} = \frac{\lambda}{2sin\theta} \quad (4)$$

$$\frac{1}{d_{hkl^2}} = \frac{4}{3}\left(\frac{h^2+hk+k^2}{a^2}\right) + \frac{l^2}{c^2} \quad (5)$$

The calculated lattice parameters for undoped and various wt.% In_2O_3 doped $LiTaO_3$ thin films are tabulated in Table 3. From the data in Table 3, the calculated lattice parameters were slightly different from the JCPDS data due to differences in annealing temperature. The data also showed that the lattice parameters increased with increasing doping concentration.

Table 1 R-profile, Goodness of Fit and crystallinity index of $LiTaO_3$ thin films doped with In_2O_3

Sample	R_{wp}	R_{exp}	GOF	Crystallinity Index (%)
$LiTaO_3$	25.7	21.8	1.39	68.53
$LiTaO_3$ + 2 wt.% In_2O_3	43.1	28.82	2.24	51.06
$LiTaO_3$ + 4 wt.% In_2O_3	18.7	10.94	2.91	88.98
$LiTaO_3$ + 6 wt.% In_2O_3	34.4	23.68	2.11	65.32

Table 2 Crystallite size, dislocation density, and lattice strain of $LiTaO_3$ thin films doped with In_2O_3

Sample	Diffraction plane	2θ (deg)	FWHM (deg)	Crystallite size (nm)	Dislocation density (cm^{-2}) x 10^{10}	Lattice strain x 10^{-3}
$LiTaO_3$	0 1 2	24.186	0.160	50.805	3.874	3.257
	1 0 4	33.293	0.197	42.001	5.669	2.881
$LiTaO_3$ + 2 wt.% In_2O_3	0 1 2	24.217	0.167	48.638	4.227	3.398
	1 0 4	33.333	0.197	42.016	5.665	2.877
$LiTaO_3$ + 4 wt.% In_2O_3	0 1 2	24.131	0.160	50.685	3.893	3.272
	1 0 4	33.231	0.189	43.834	5.204	2.765
$LiTaO_3$ + 6 wt.% In_2O_3	0 1 2	24.187	0.158	51.408	3.784	3.218
	1 0 4	33.293	0.178	46.620	4.601	2.596

Table 3 Lattice parameter values of $LiTaO_3$ thin films doped with In_2O_3 hexagonal structure

Lattice parameter	$LiTaO_3$	$LiTaO_3$ + 2 wt.% In_2O_3	$LiTaO_3$ + 4 wt.% In_2O_3	$LiTaO_3$ + 6 wt.% In_2O_3	JCPDS (Natl Bur, 1977)

c (Å)	13.658	13.643	13.676	13.658	13.755
a (Å)	5.038	5.032	5.051	5.038	5.153

3.2 Optical properties

The optical properties of the undoped and In_2O_3 doped $LiTaO_3$ thin films were investigated by analyzing the reflectance spectra in the wavelength between 230 nm and 850 nm (UV-Vis range). The reflectance spectra of the synthesized films are shown in Figure 2. In the reflectance spectra, it is observed that the films have low reflectance in the ultra-violet range and high reflectance in the visible range. The band gap energy (Eg) values of the synthesized films could be estimated from the reflectance spectra. The recorded reflectance spectra were first transformed to the absorption spectra by applying the Kubelka-Munk function (F(R)). Then, the Tauc plot method is employed to determine the band gap energy [5,9,35]. The Kubelka-Munk function and the Tauc formula are given in Eq. 6 and Eq. 7, respectively.

$$F(R) = \frac{K}{S} = \frac{(1-R)^2}{2R} \propto \alpha_{K-M} \quad (6)$$

$$(\alpha_{K-M} h\nu)^{1/n} = B(h\nu - Eg) \quad (7)$$

K and S are absorption and scattering coefficients, respectively. R is reflectance value, hv is the photon's energy, B is a constant, Eg is the band gap energy, and n is the nature of the electron transition (= ½ for direct transition band gap).

From the Tauc plot, it is found that the optical band gap energy of undoped, 2 wt.%, 4 wt.%, and 6 wt.% In_2O_3 doped $LiTaO_3$ thin films are 5,034 eV, 5,079 eV, 5.122 eV, and 5,184 eV, respectively, as shown in Figure 3. From the data, it was observed that the increase in doping concentration also increase the band gap energy of the films. This result is parallel agreement to Singh et al. [40].

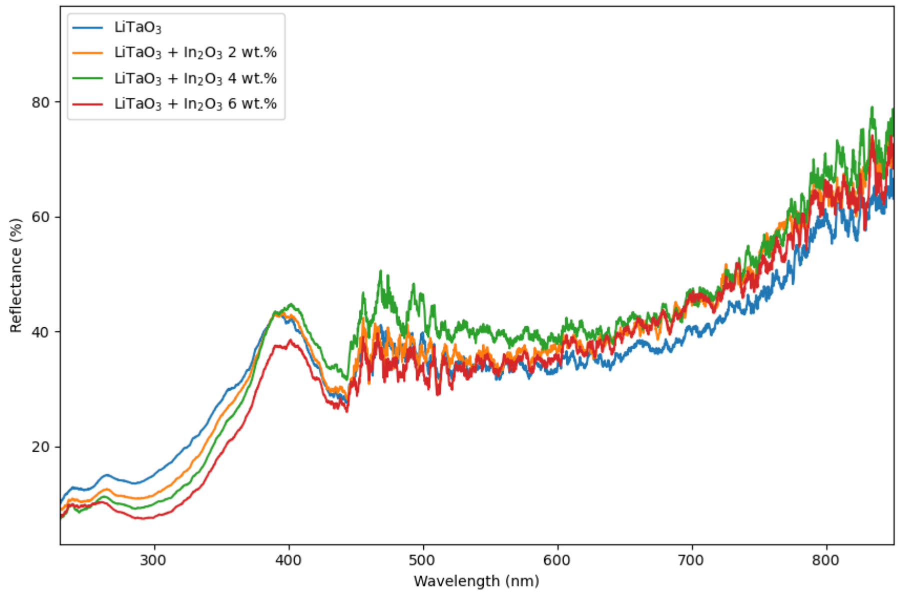

Figure 2. Reflectance spectra of $LiTaO_3$ thin films

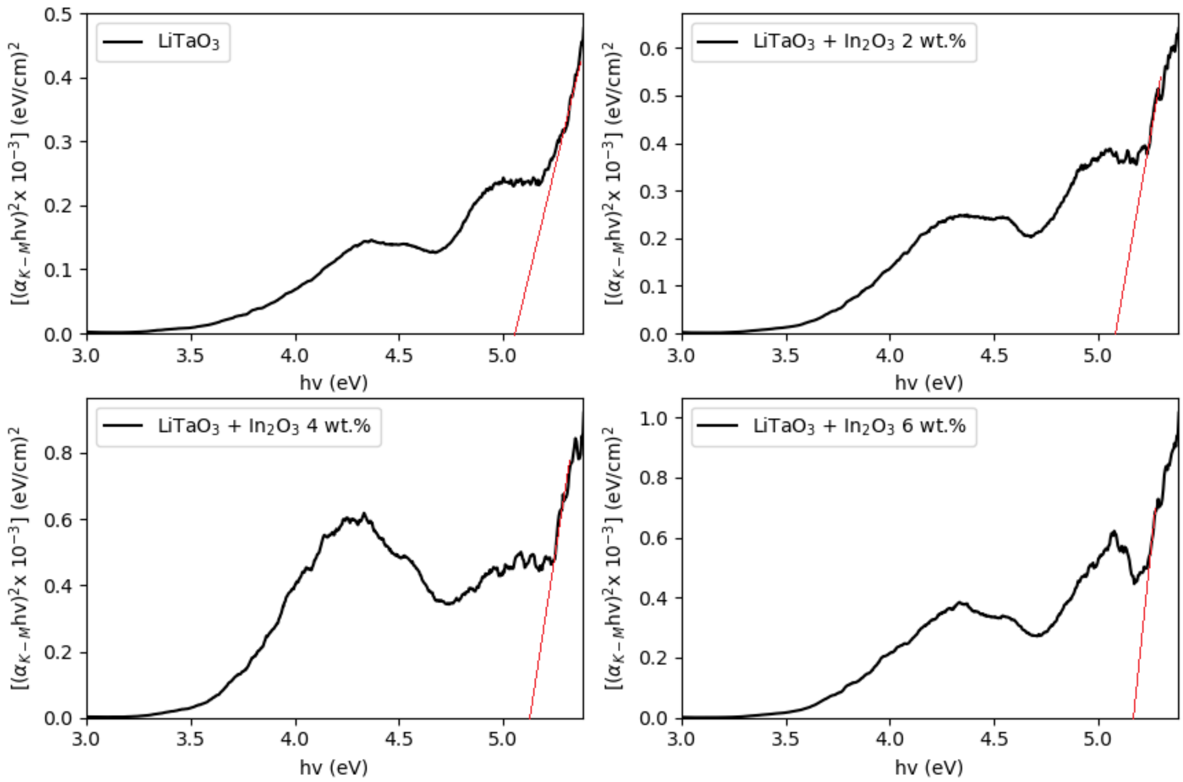

Figure 3. Energy band gap of $LiTaO_3$ thin films

Refractive index (n_e) of the films were obtained by using Sellmeier formula [9,36,37]:

$$n_e{}^2(\lambda,T) = A + \frac{B+b(T)}{\lambda^2-[C+c(T)]^2} + \frac{E}{\lambda^2-F^2} + \frac{G}{\lambda^2-H^2} + D\lambda^2 \quad (8)$$

where λ is the wavelength related to the band gap energy value, b(T), c(T) is the temperature dependent, and A, B, C, D, E, F, G, H are the coefficients of Sellmeier. The data show that the value of the refractive index also increases as the band gap energy increased. The refractive index, band gap energy and related color spectra of undoped, 2 wt.%, 4 wt.%, and 6 wt.% In_2O_3 doped $LiTaO_3$ thin films were listed in Table 4. The result was acceptable as previous study by Zielinska et al. [30].

Table 4 The energy gap and the refractive index of $LiTaO_3$ thin films

Sample	Band gap (eV)	Wavelength (nm)	Color spectra	Refractive index
LiTaO3	5.034	246.855	ultraviolet	1.70364373
LiTaO3 + 2 wt.% In2O3	5.079	244.692	ultraviolet	1.70364374
LiTaO3 + 4 wt.% In2O3	5.122	242.529	ultraviolet	1.70364375
LiTaO3 + 6 wt.% In2O3	5.184	239.715	ultraviolet	1.70364377

3.3 Raman Spectrum

Raman spectrum of $LiTaO_3$ single crystals with various stoichiometric was used to investigate the compositional uniformity of the crystals [11,12,18]. The first principles, the peaks of Raman intensity were assigned by referring to the mode energy [12,33,34]. The phonons identification may become complicated because some Raman intensity might be lost on the calculated modes [12]. Longitudinal phonon mode was observed when polarization vectors and phonon wave vector are parallel, whereas transversal phonon mode was observed when polarization vectors and phonon wave vector are perpendiculars.

Figure 4 shows the Raman spectrum of undoped, 2 wt.%, 4 wt.%, and 6wt.% In_2O_3 doped $LiTaO_3$ thin films. In this experiment, Raman spectra were obtained by Raman spectroscopy in the range of 100 to 1000 cm^{-1}.

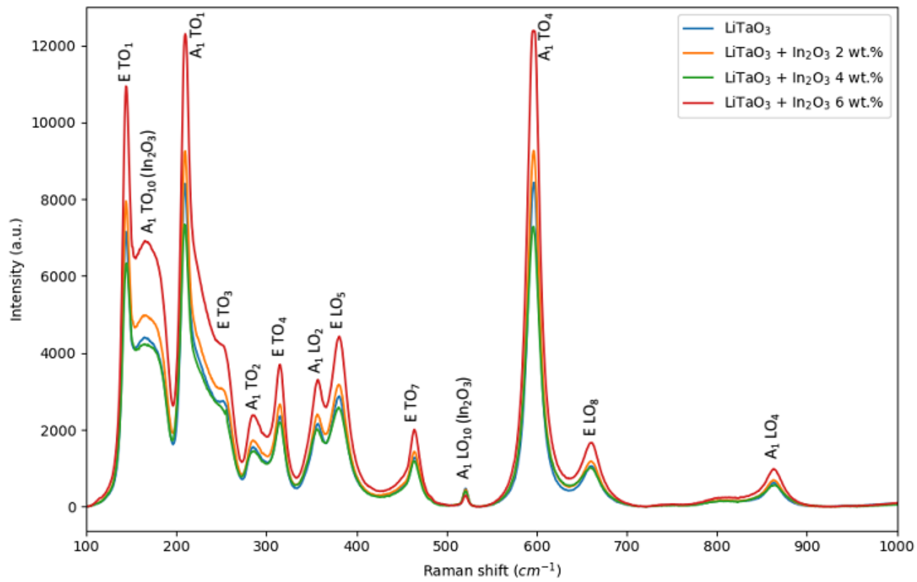

Figure 4. Raman spectroscopy of $LiTaO_3$

Table 5 shows the result of active phonon frequencies of undoped, 2%, 4%, and 6% In_2O_3 doped $LiTaO_3$ thin films. The experiment results show that the most significant deviation is 5 cm^{-1} at A_1 TO_4 and the mean deviation is 1.82 cm^{-1}.

Table 5 Theory and experiment result of active phonon frequencies of $LiTaO_3$

Symmetry	Mode	Exp.	Literature [9]	Mode	Exp.	Literature [9]
A1	TO1	209	209	LO1		255
A1	TO2	285	286	LO2	356	355
A1	TO3		376	LO3		403
A1	TO4	596	591	LO4	863	866
E	TO1	144	144	LO1		190
E	TO2		199	LO2		
E	TO3	253	253	LO3		279
E	TO4	315	319	LO4		
E	TO5		409	LO5	380	381
E	TO6		420	LO6		453
E	TO7	463	459	LO7		
E	TO8		590	LO8	661	660
E	TO9		669	LO9		866
A1	TO10	165		LO10	521	

Phonon activities in hexagonal crystal structures (XRD analysis) and electron jump from valence band into induction band to become free electron (UV-Vis analysis) leads to the occurrence of transversal and longitudinal mode (Raman spectroscopy) and electron free radicals on the thin film surface. The intensity difference of the free radicals shown in Raman spectroscopy (Figure 4) is caused by In^{3+} doping and radius in the $LiTaO_3$ thin films. For both undoped and In_2O_3 doped $LiTaO_3$ thin films, the experiment results of active phonon frequencies are in good agreement with the literature [12].

4. CONCLUSION

The formation of In_2O_3 doped $LiTaO_3$ thin films with CSD method was succeeded. Analysis of the thin films was conducted using XRD, UV-Vis spectrometer and Raman spectroscopy. The XRD patterns show that the structural properties of $LiTaO_3$ thin film are affected by the indium doping, where the increase in doping concentration causes an increase of crystallite size and lattice parameter values. The reflectance spectrum showed that the films have low reflectance in the ultra-violet range, with the refractive index between 1.70364373 and 1.70364377 for undoped film and 6 wt.% In_2O_3 doped film, respectively. The Tauc plot results show that increasing the doping concentration also increases the film band gap energy. The Raman results show that the most significant deviation is 5 cm^{-1} (A_1TO_4) for the 4 wt.% In_2O_3 doped film. Based on the characterization result, it can be concluded that the $LiTaO_3$ thin films are very promising for application as a light sensor, especially in the ultraviolet region, where 6 wt.% In_2O_3 doped film shows best figure of merit.

ACKNOWLEDGEMENTS

This study was supported by the Ministry of Research, Technology and Higher Education of the Republic of Indonesia through the Research Grant No. 004/AKM/MONOPNT/2019.

REFERENCES

[1] Garraud, A., Nadar, S., Giani, A., Combette, P., "Self-Polarized Pyroelectric $LiTaO_3$ thin films," DTIP, Cannes Cote d'Azur, France, (2014).

[2] Casson, J. L., Gahagan, K. T., Scrymgeour, D. A., Jain, R. K., Robinson, J. M., Gopalan, V., Sander, R. K., J. Opt. Soc. Am. B, vol. 21, no. 11 (2004) pp. 1948-1952.

[3] Gou, J., Wang, J., Huang, Z. H., and Jiang, Y.D., Key Engineering Materials. vols 531-532 (2013) pp. 446-449.

[4] Norkus, V, "Pyroelectric infrared detectors based on lithium tantalate: state of the art and prospects," *Proceedings of SPIE*. vol. 5251 (2004) pp. 121-128.

[5] Djohan, N., Estrada, R., Sevani, N., Hardhienata, H., and Irzaman, "The Optical Band Gap Based on K-M Function on layer of $LiTaO_3$ with Variation Treatment of Annealing Temperature," ICSGTEIS (2018).

[6] Estrada, R., Djohan, N., Pasole, D., Dahrul, M., Kurniawan, A., Iskandar, J., Hardhienata, H., and Irzaman, "The optical band gap of $LiTaO_3$ and Nb_2O_5 – doped $LiTaO_3$ thin films based on Tauc Plot method to be applied on satellite," *IOP Conf. Ser.: Earth Environ. Sci.,* vol 54 (1), (2017), No. article 012092.

[7] Zhang, D. Y., Huang, D. G., Li, J. H., Li, K., Dan, D. D. and Dong, Z., *Journal of Infrared and Millimeter Waves,* vol. 26 (2007) No. 3, p. 170 (In Chinese).

[8] Mendoza, S. D. V., Momaca, J. T. H., Galindo, J. T. E., Flores, D. M. C., Mendez, S. F. D., Mancilla, J. R. F., Crystals, vol. 10, no. 50 (2020).

[9] Djohan, N., Estrada, R., Sevani, N., Hardhienata, H., and Irzaman "Crystalline Structure and optical properties of thin film $LiTaO_3$," *IOP Conf Ser.: Earth Environ*. (2019), Sci. 284012039.

[10] Fakhri, M. A., Douri, Y. A., Hashim, U., Salim, E. T., Solar Energy. vol 120 (2015) pp. 381–388.

[11] Kastritskii, S. M., Aillerie, M., Bourson, P., Kip, D., *Applied Physics B.* vol 95 (2009) pp. 125-130.

[12] Sanna, S., Neufeld, S., Rűsing, M., Berth, G., Zrenner, A., and Schmidt W. G., *Physical Review B. vol 91,* (2015) pp. *224302*.

[13] Buixaderas, E., Gregora, I., Savinov, M., Hlinka, J., Jin, L., Damjanovic, D. and Malic, B., *Phys Rev B. vol 91,* (2015) pp. *014104.*

[14] Irzaman., Pebriyanto, Y., Apipah, E. R., Noor, I., Alkadri A., *Integrated Ferroelectrics*. vol 167, (2015) pp.137-145.

[15] Bartasyte, A., Margueron, S., Kreisel, J., Bourson, P., Chaix-Pluchery, O., Rapenne-Homand, L., Santiso, J., Jimenez, C., Abrutis, A., Weiss, F., and Fontana, M. D., *Phys Rev B. vol 79,* (2009) pp. *104104*.

[16] Mouras, R., Fontana, M. D., Bourson, P., and Postnikov, A. V., *J. Phys.: Condens. Matter. vol 12 (2000) pp. 5053–5059.*

[17] Quispe-Siccha, R., Mejfa-Uriarte, E. V., Villagran- Muniz, M., Jaque, D., Garcia Solé, J., Jaque, F., Sato-Berrú, R. Y., Camarillo, E., Hernández A. J., and Murrieta S. H., J. Phys.: Condens. Matter. vol 21, (2009) pp. 145401.

[18] Repelin, Y., Husson, E., Bennani, F., Proust, C., *Journal of Physics and Chemistry of Solids*. vol 60 (1999) pp. 819-825.

[19] Djohan, N., Estrada, R., Sari, D., Dahrul, M., Kurniawan, A., Iskandar, J., Hardhienata, H., and Irzaman, "The effect of annealing temperature variation on the optical properties test of $LiTaO_3$ thin films based on Tauc Plot method for satellite technology," *IOP Conf. Ser.: Earth Environ. Sci,* vol. 54, (2017), No. article 012093.

[20] Zelenovskiy, P. S., Shur, V. Y., Bourson, P., Fontana, M. D., Kuznetsov, D. K., and Mingaliev, E. A., *Ferroelectrics*. vol 398, (2010) pp. 34-41.

[21] Fontana, M. D., Hammoum, R., Bourson, P., Margueron, S., and Shur, V. Y., *Ferroelectrics.* vol 373, (2008) pp. 26-31.

[22] Berth, G., Hahn, W., Wiedemeier, V., Zrenner, A., Sanna, S., and Schmidt, W. G., *Ferroelectrics*. vol 420, (2011) pp. 44-48.

[23] Sanna, S., Berth, G., Hahn, W., Widhalm, A., Zrenner, A., and Schmidt, W. G., *Ferroelectrics*. vol 419, (2011) pp. 1-8.

[24] Irzaman., Siskandar, R., Nabilah, N., Aminullah, Yuliarto, B., Hamam, K. A., and Alatas, H., *Ferroelectrics*. vol 524, (2018) pp. 44-55.

[25] Irzaman., Sitompul, H., Masitoh., Misbakhusshudur, M., and Mursyidah., *Ferroelectrics*. vol 502, (2016) pp. 9-18.

[26] Irzaman., Siskandar, R., Aminullah., Irmansyah., and Alatas, H., *Integrated Ferroelectrics*. vol 168, (2016) pp. 130-150.

[27] Irzaman., Putra, I. R., Aminullah., Syafutra, H., Alatas, H., Procedia Environmental Sciences. vol 33, (2016) pp. 607-614.

[28] Djohan, N., Estrada, R., Sari, F. I. W., Kurniawan, A., Iskandar, J., Dahrul, M., Hardhienata, H., and Irzaman., "Classification of undoped and 10% Ga_2O_3-doped $LiTaO_3$ thin films based on electrical conductivity and phase characteristic," *ARPN J. Eng. Appl. Sci*., vol 12 (2017), pp. 3779-3782.

[29] Estrada, R., Djohan, N., Rundupadang, G. C., Kurniawan, A., Iskandar, I., Dahrul, M., Hardhienata, H., and Irzaman., "Electrical Properties Test of Dielectric Constant and Impedance Characteristic Thin Films of $LiTaO_3$ and 10% Ga_2O_3-doped $LiTaO_3$," *ARPN Journal of Engineering and Applied Sciences.* vol 12, (2017) pp. 3813-3816.

[30] Zielińska, B., Mijowska, E., Kalenczuk, R. J., *Materials Characterization.* vol 68 (2012), pp. 71-76.

[31] Kassim, A., Nagalingam, S., Min, H. S., and Karrim, N., *Arabian Journal of Chemistry*. vol 3, (2010) pp. 243-249.

[32] Rajesh, D., and Sunandana, C. S., *Result in Physics*. vol 2, (2012) pp. 22-25.

[33] Parlinski, K., Li, Z. Q., and Kawazoe, Y., *Phys. Rev. B,* vol *61,* (2000) pp. *272*-278.

[34] Casiuc, V., Postnikov, A. V., and Borstel, G., *Phys. Rev. B* vol *61,* (2000) pp. *8806*.

[35] Mulyadi., Rika, W., Sulidah., Irzaman., and Hardhienata, H., "Barium Strontium Titanate Thin Film Growth with rotational speed variation as a satelite temperature sensor prototype," *IOP Conf. Ser.: Earth Environ.* (2017) *Sci.* 54 012094.

[36] Bruner, A., Eger, D., Oron, M. B., Blau, P., and Katz, M., *Opt. Lett.* vol 28, (2003) pp. 194*.*

[37] Weng W -L, Liu Y -W, Zhang X -Q 2008 Temperature-dependent Sellmeier Equation for 1.0 mol % Mg-Doped Stoichiometric Lithium Tantalate *Chin. Lett. 25 4303.*

[38] Salah, M., Azizi, S., Boukhachem, A., Khaldi, C., Amlouk, M., Lamloumi, J., Applied Physics A, vol. 125, no. 615 (2019).

[39] Sahoo, B., Behera, D., Pradhan, S. K., Mishra, D. K., Sahoo, S. K., Nayak, R. R., Sekhar, K. P. C., Mater. Res. Express, vol. 6, 1150a6 (2019), pp. 1-13.

[40] Singh, G., Shrivastava, S. B., Jain, D., Pandya, S., Shripathi, T., Ganesan, V., Bull. Mater. Sci., vol. 33, no. 5 (2010), pp. 581-587.